



Empirical estimation of size-resolved scavenging coefficients derived from *in-situ* measurements at background sites in Korea during 2013–2020

Yongjoo Choi^{a,*}, Chang Hoon Jung^b, Junyoung Ahn^{c,*}, Seung-Myung Park^c, Kyung Man Han^d, Jongbyeok Jun^a, Giyeol Lee^a, Jiyoung Kim^c, Yongjae Lim^c, Kyeong-Sik Kang^c, Ilkwon Nam^{a,c}, Sumin Kim^c

^a Department of Environmental Science, Hankuk University of Foreign Studies, Gyeonggi 17035, Republic of Korea

^b Department of Health Management, Kyungin Women's University, Incheon 21041, Republic of Korea

^c Climate and Air Quality Research Department, National Institute of Environmental Research, Incheon 22689, Republic of Korea

^d School of Earth Science and Environmental Engineering, Gwangju Institute of Science and Technology, Gwangju 61005, Republic of Korea

ARTICLE INFO

Keywords:

Aerosol
Below-cloud scavenging coefficients
Wet removal
Long-term measurements
Empirical equation

ABSTRACT

Owing to insufficient detailed in-field observations for explaining and quantifying the wet-scavenging coefficients, especially those below-cloud (Λ_{below}), prediction of accurate aerosol concentrations and/or behaviors in the atmosphere remains challenging. As a pioneering effort, this study focused on establishing an empirical equation for size-resolved Λ_{below} , which represent the characteristics in Korea, using long-term aerosol number size distribution and meteorological variable measurements at two background sites in Korea (Baengnyeong and Jeju). The median Λ_{below} values derived from the total number concentrations were $8.06 \times 10^{-6} \text{ s}^{-1}$ for Baengnyeong and $1.04 \times 10^{-5} \text{ s}^{-1}$ for Jeju, which are similar to or slightly lower than the Λ_{below} reported by previous *in-situ* studies. These may be caused by differences in the precipitation rates, precipitation drop sizes, aerosol chemical/hygroscopic properties, and aerosol size distributions at the measurement sites. Although the derived parameterization can cover a wide range (10 nm to 10 μm), the derived equation for the fourth-degree polynomial shows a high correlation coefficient of 0.81, indicating that the measured and fitted Λ_{below} converge within a narrow range. Moreover, the variation in Λ_{below} is relatively constant for aerosol diameters larger than $\sim 1 \mu\text{m}$, similar to those derived from theoretical equations rather than empirical equations in previous studies. This study is thus expected to contribute to improving the below-cloud scavenging module implemented in a chemical transport model by covering a wide range of aerosol diameters to avoid overestimation by extrapolation of Λ_{below} .

1. Introduction

Aerosols in the atmosphere are mainly removed by wet deposition, which is a key mechanism for mitigating air pollution (Seinfeld and Pandis, 2016), and includes the below-cloud (i.e., washout) and in-cloud (i.e., rainout) processes (Andronache, 2003; Choi et al., 2020b; Feng, 2007; Jung et al., 2022; Ryu and Min, 2022; Wang et al., 2010; Wu et al., 2022; Xu et al., 2017; Zhang et al., 2013). Textor et al. (2006) compared the aerosol removal processes in different global chemical transport models (CTMs) and determined that wet removal is a dominant sink for anthropogenic aerosols (e.g., sulfates, black carbon, and primary organic matter) on the global annual scale. Below-cloud scavenging has been identified as one of the most efficient removal mechanisms for

atmospheric aerosols and is thus a key process in the CTM (Andronache, 2003; Jung et al., 2022; Textor et al., 2006; Wang et al., 2014; Wu et al., 2022). The contribution of below-cloud scavenging to the total wet deposition ranges from 50% to 60% in north China (Ge et al., 2021; Xu et al., 2017), $\sim 40\%$ in Korea and Japan (Choi et al., 2020b), and $\sim 80\%$ in India (Chatterjee et al., 2010) based on field measurements.

However, the wet scavenging process is still insufficient for predicting the atmospheric aerosol concentration owing to the difficulty of accurately evaluating the wet removal process (Croft et al., 2010; Grythe et al., 2017; Luo et al., 2020; Wang et al., 2014). There are insufficient *in-situ* detailed observations that explain and quantify the interactions between aerosols and cloud particles at the microscale, which hinders better understanding of the physical processes (Ding et al., 2019). A

* Corresponding authors.

E-mail addresses: choingjoo@hufs.ac.kr (Y. Choi), nierair@korea.kr (J. Ahn).

<https://doi.org/10.1016/j.atmosres.2023.106971>

Received 17 March 2023; Received in revised form 17 July 2023; Accepted 22 August 2023

Available online 26 August 2023

0169-8095/© 2023 Elsevier B.V. All rights reserved.

parameter called the scavenging coefficient (Λ) is used to determine the fraction of aerosols removed per unit time (s^{-1}) by hydrometeors and is typically used when solving for wet removal processes in various CTMs (Seinfeld and Pandis, 2016; Wang et al., 2014; Xu et al., 2017). In particular, the below-cloud scavenging coefficient (Λ_{below}) is affected by rain droplet-size distribution, precipitation intensity, and collision efficiency between the aerosols and rain droplets as well as the chemical properties of aerosols and their atmospheric concentrations (Chate et al., 2003; Laakso et al., 2003; Zhang et al., 2013), which prevents accurate simulation of the particulate matter (PM) to assess air quality, climate, and/or the ecosystem. Therefore, using different formulations for Λ can produce significantly different predictions of aerosol behaviors over the regional/global scales (Ryu and Min, 2022).

Several studies have attempted to derive the equation for Λ_{below} from both field measurements (Andronache et al., 2006; Baklanov and Sørensen, 2001; Jylhä, 1991; Laakso et al., 2003; Pryor et al., 2016; Xu et al., 2019; Xu et al., 2017) and theoretical estimations (Andronache, 2003; Henzing et al., 2006; Jung et al., 2022; Wang et al., 2010). However, Λ_{below} derived from field measurements varies by one to two orders of magnitude than those derived by theoretical calculations for accumulation-sized aerosols (diameter of aerosol (d_a) of $0.1 \leq d_a \leq 1 \mu\text{m}$) (Jones et al., 2022; Luo et al., 2020; Luo et al., 2019; Wang et al., 2014). Recently, enhanced Λ_{below} has been obtained from actual atmospheric measurements owing to contributions from in-cloud scavenging and other confounding atmospheric processes, such as turbulent diffusion and convective cloud process, which is difficult when considering only the effects of Λ_{below} (Andronache et al., 2006; Wang et al., 2011).

It should be noted that Λ_{below} shows large spatial and temporal variations when derived experimentally due to differences in the characteristics of aerosols and meteorological variables depending on the measurement sites (Andronache et al., 2006; Jones et al., 2022; Pryor et al., 2016). Regionally limited to Asia, Λ_{below} based on field observations has been investigated in background areas, such as Baengnyeong and Gosan in Korea as well as Noto in Japan (Choi et al., 2020b), to polluted areas, such as Beijing and North China Plain in China (Ge et al., 2021; Hu et al., 2005; Xu et al., 2019; Xu et al., 2017) and India (Chakraborty et al., 2016; Rajeev et al., 2016). Despite the increased number of size-resolved Λ_{below} from field observations in recent decades (e.g. Blanco-Alegre et al., 2021; Blanco-Alegre et al., 2018; Cugerone et al., 2018; Xu et al., 2019), to the best of the authors' knowledge, there are very few observational studies on Λ_{below} that cover the sub-micron ($\sim 10 \text{ nm}$) to super-micron ($\sim 10 \mu\text{m}$) range along with consideration of a sufficient number of precipitation samples (~ 100) to parameterize statistically robust estimates of the size-resolved Λ_{below} (Laakso et al., 2003; Pryor et al., 2016; Zikova and Zdimal, 2016). Moreover, only Laakso et al. (2003) and Pryor et al. (2016) have attempted to develop empirical parameterizations for the size-resolved Λ_{below} by covering aerosol sizes from 10 to 500 nm depending on the precipitation rates; thus, there is a lack of information regarding Λ_{below} above super-micron aerosol sizes from *in-situ* measurements.

Considering the importance of the size-resolved empirical equation of Λ_{below} for wet deposition in CTMs and the limited observation data available for East Asia, the representativeness of the empirical equations proposed by Laakso et al. (2003) and Pryor et al. (2016) should be validated, and more advanced formulations derived from long-term measurements must be evaluated. Hence, to establish below-cloud scavenging characteristics representative of the Korean peninsula, the empirical equation for size-resolved Λ_{below} was derived using long-term (8 years) measurements of the aerosol number size distribution over a wide range of aerosol sizes (nanometer to micron) and precipitation intensities at two background sites in Korea (Baengnyeong and Jeju). The differences in the aerosol number size distributions between Baengnyeong and Jeju as aspects of the total and monthly averages are discussed in Sections 3.1 and 3.2, respectively. Thereafter, the size-resolved Λ_{below} depending on the precipitation rate and the newly derived size-resolved Λ_{below} formula are explored in Sections 3.3 and

3.4, respectively, to establish the representativeness of the Λ_{below} empirical formula over East Asia.

2. Methods

2.1. Study region

Fig. 1 shows the geophysical locations of the two measurement sites, Baengnyeong (37.96°N, 124.63°E) and Jeju (33.35°N, 126.39°E), which are the representative background sites in Korea. Both sites have intensive measurement stations that are operated by the National Institute of Environmental Research (NIER) in Korea. Baengnyeong is located on a relatively small and low-lying island off the northwestern boundary of Korea; it is frequently influenced by various types of aerosols (photochemically aged, less-oxidized transported industrial emissions, biomass burning, and dust) from mainland China and the Korean peninsula (Boris et al., 2016; Lee et al., 2015; Park et al., 2022). Jeju island is located off the southern part of Korea and is frequently affected by air masses from East China and South Korea (Choi et al., 2020a; Choi et al., 2020b); the measurement site is on a hilly and mountainous region separating two urban areas ($\sim 20 \text{ km}$ each from the centers of Jeju city (population: 39,000) and Seogwipo city (population: 1.05 million)); there are no major emission sources nearby because the sampling site is located in a rural area with low-rise buildings and scattered farmlands, except for a few golf courses nearby.

For the meteorological variables (precipitation amount, wind speed, wind direction, temperature, and relative humidity), hourly measurements from the nearest weather stations (i.e., automated synoptic observing system (ASOS) or auto weather station (AWS)) to these sites were used. The ASOS and AWS are operated by the Korea Meteorological Administration (KMA). For the Baengnyeong site, the ASOS (37.97°N, 124.63°E) was selected because of its location of about 200 m north of the measurement site. On the other hand, for Jeju, the closest ASOS is in Jeju city, which is 20 km north of the measurement site; thus, the AWS was selected for Jeju after considering its distance from the measurement site and available long-term meteorological data measurements. As a result, Segwang AWS (No. 752) was selected because the No. 883 AWS has a relatively short period of data after 2016 despite being closer to the measurement site (3.5 km for No. 883 vs. 9 km for No. 752). The Pearson's correlation coefficient (R) of the hourly precipitations between the two AWS sites was 0.87 and that of the best-fit line was 0.96, indicating that local differences based on distance may be neglected.

2.2. Measurements of the aerosol number size distributions

The size-resolved aerosol number size distributions were measured using a combined scanning mobility particle sizer (SMPS; model 3936, TSI, Shoreview, MN, USA) and an aerodynamic particle sizer (APS; model 3321, TSI, Shoreview, MN, USA). The SMPS can measure 54 size classes over the mobility diameter range of 10–470 nm using an electrostatic classifier (TSI 3080), a long differential mobility analyzer (TSI DMA3081), and a condensation particle counter (TSI 3025A) (Kim et al., 2016; Kim et al., 2013). The aerodynamic diameter range measured by the APS was 0.54–20 μm using the time-of-flight technique (Baron, 1986). The measurement interval for both the SMPS and APS was 5 min under operation with an aerosol flow rate of 0.5 L min^{-1} and a sheath airflow rate of 5.0 L min^{-1} . Because the mobility equivalent diameter for the SMPS and aerodynamic diameter for the APS have different definitions, the mobility diameter from the SMPS was converted to aerodynamic diameter by applying Eq. (1):

$$d_{\text{aero}} = d_m \times \sqrt{\rho_a / \chi \rho_0} \quad (1)$$

where d_{aero} and d_m are the aerodynamic and mobility equivalent diameters, respectively; ρ_0 is the reference density (1 g cm^{-3}); χ is the shape factor equal to 1 (Khlystov et al., 2004; Si et al., 2018). The aerosol

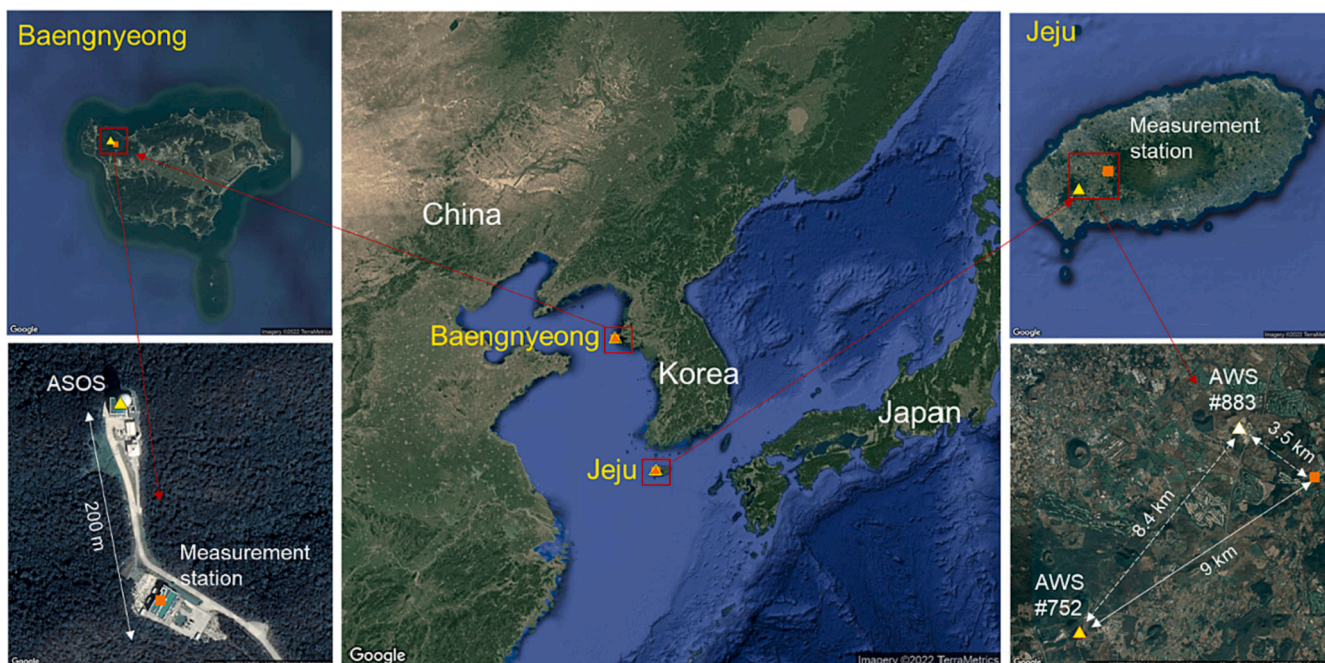


Fig. 1. Locations of the two intensive measurement stations (Baengnyeong and Jeju; orange squares) in this study. These sites are the representative background sites in South Korea. The yellow triangles indicate the locations of the nearest meteorological stations to the measurement sites. (For interpretation of the references to colour in this figure legend, the reader is referred to the web version of this article.)

dry density (ρ_a) was assumed as 1.4 g cm^{-3} , which represents both urban and rural aerosols (Rissler et al., 2014). It should be noted that the effect of differences in the assumed ρ_a is negligible because the mean absolute percentage error of the results is $<1\%$.

Owing to the possibility of low sampling efficiency of the APS at small sizes (Beddows et al., 2009), only APS data at sizes above 600 nm are used here; nevertheless, there is still a discontinuity issue when merging the aerosol number size distributions between the SMPS and APS. Therefore, the influence of the discontinuities could be minimized using an R function for cubic spline interpolation (Lee et al., 2021). Then, only aerosol sizes $<10 \mu\text{m}$ are considered to avoid errors from the insignificant changes in the aerosol number concentrations because large aerosols ($d_a > 10 \mu\text{m}$) are almost always numerically limited to less than ten. The total amount of hourly data was 70,128; by season, there were 15,757 (16,543), 12,500 (14,517), 15,146 (15,749), and 14,265 (15,752) from Baengnyeong (Jeju) for spring, summer, fall, and winter, respectively; compared to the possible amounts of data from the full operation of the SMPS, these values correspond to 90% (94%), 71% (83%), 86% (90%), and 81% (90%) for Baengnyeong (Jeju) for each season and 82% (89%) in total. Therefore, most SMPS and APS measurements proceed smoothly regardless of the season during the measurement periods.

2.3. Scavenging coefficient

The *in-situ* measured aerosol number size distributions and precipitation rates are used to derive the size-resolved scavenging coefficients ($\Lambda(d_a)$) via Eq. (2):

$$-\frac{dN(d_a)}{dt} = \Lambda(d_a) \quad (2)$$

where d_a is the aerosol diameter, dt is the duration of precipitation in hour, and $dN(d_a)$ are the differences in the aerosol number concentrations of individual bin sizes before and after the precipitation event (Seinfeld and Pandis, 2016). When assuming that aerosol removal occurs only by precipitation, $\Lambda_{\text{below}}(d_a)$ evolves as in Eq. (3), as given by Laakso et al. (2003) and Pryor et al. (2016):

$$\Lambda_{\text{below}}(d_a) = -\frac{1}{t_1 - t_0} \ln \left(\frac{N_1(d_a)}{N_0(d_a)} \right) \quad (3)$$

where t_1 and t_0 are the time instances of two subsequent measurements, and N_1 and N_0 are the number concentrations of d_a at the corresponding instances. In this study, Λ_{below} was calculated based on 1-h data (i.e., $t_1 - t_0 = 3600 \text{ s}$).

2.4. Data selection criteria

According to the hourly measured meteorological parameters from the selected ASOS and AWS near the study sites, the following thresholds were applied to acquire reliable data from the entire dataset. First, to exclude any influence of scavenging by snow and errors in the rain measurements caused by frozen measurement devices, data were selected when the measurements were conducted above 0°C both before and after the precipitation events. Next, Λ_{below} was calculated by selecting hourly precipitation rates exceeding or equal to 0.5 mm h^{-1} instead of 0.4 mm h^{-1} (Laakso et al., 2003) because small amounts of precipitation may result in possible inaccuracies of the precipitation measurements at low intensities, and the threshold is the detection limit of the precipitation rate at the AWS (for the ASOS, this is 0.1 mm h^{-1}). Then, for reliable scavenging coefficient estimation, two consecutively measured air parcels must have been initially exposed to rain at the same conditions in time (beginning of rain). Therefore, to avoid changes in the aerosol number concentrations due to advection in the frontal zones, rain events with significantly changing meteorological parameters, such as absolute differences in the relative humidity ($\leq \pm 20\%$), wind speed ($\leq \pm 5 \text{ m s}^{-1}$), and wind direction ($\leq \pm 45^\circ$) (Cugeron et al., 2018), were rejected.

3. Results and discussion

3.1. Characteristics of the aerosol number size distributions at the two sites

Fig. 2 shows the median aerosol number size distributions for the two

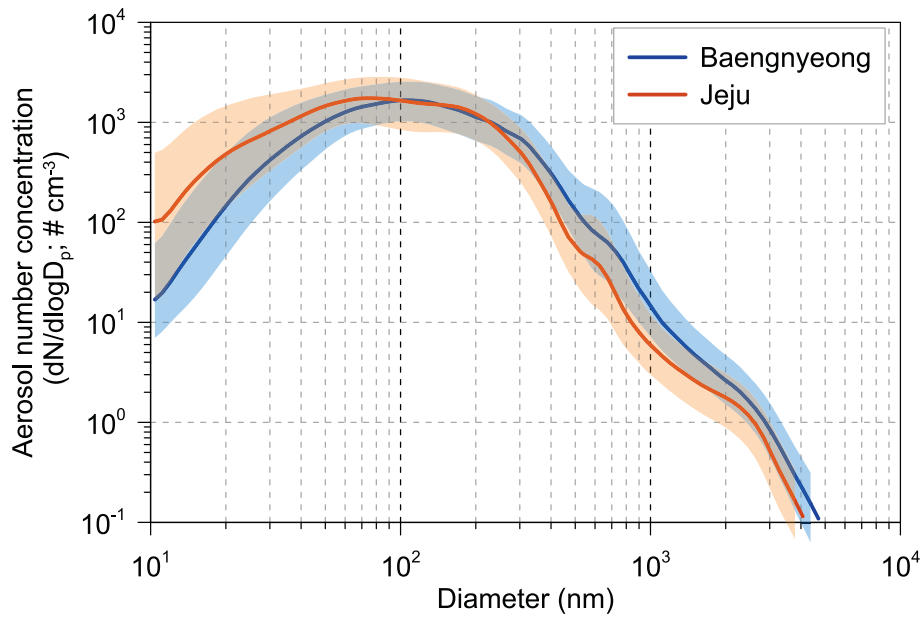


Fig. 2. Median aerosol number size distributions and number concentrations at the Baengnyeong and Jeju intensive measurement stations from 2013 to 2020. The lower and upper borders of the shaded areas indicate the 25th and 75th percentiles, respectively.

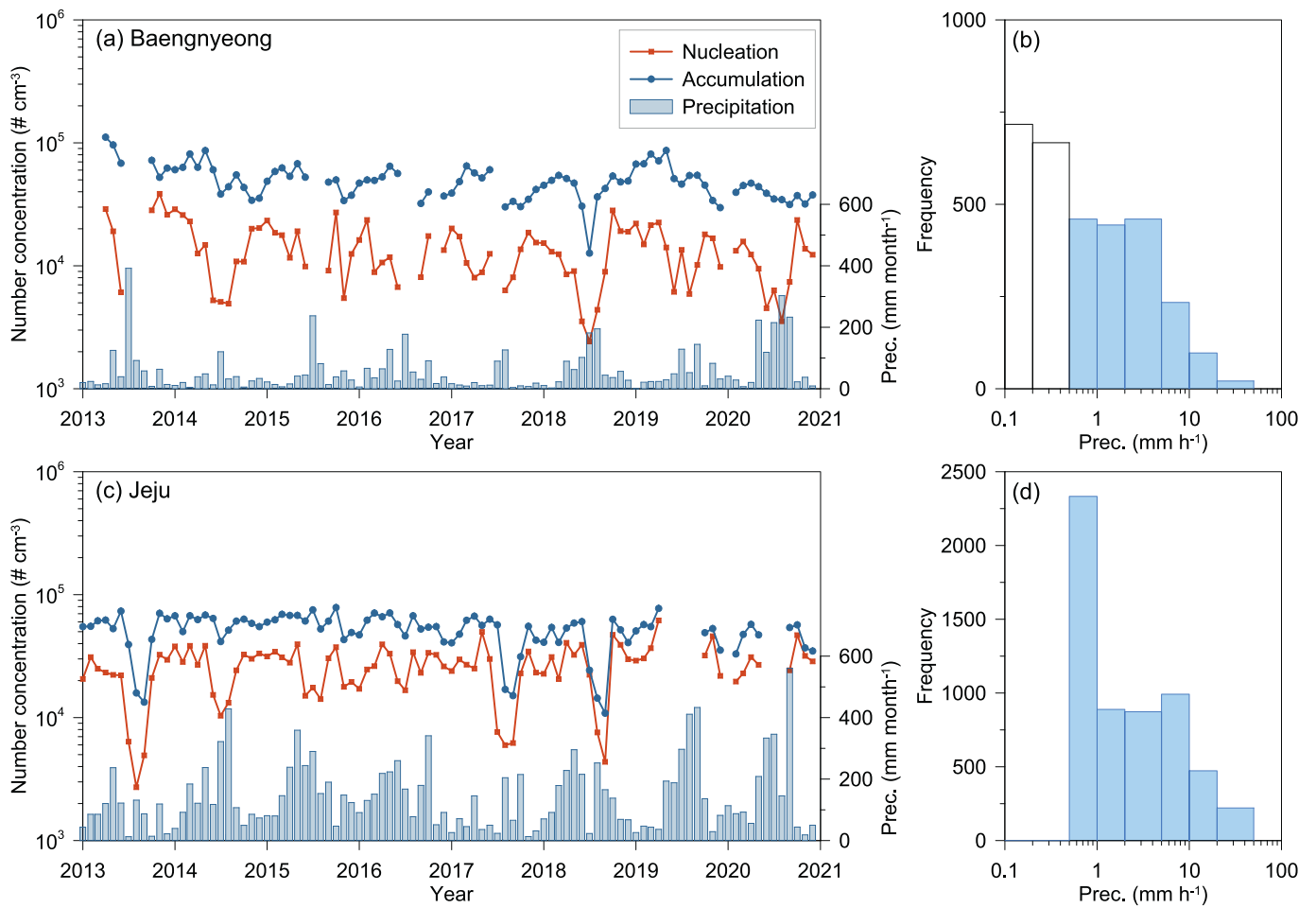


Fig. 3. Time-series data of the aerosol number concentrations and precipitation rates at Baengnyeong and Jeju from 2013 to 2020 (a and c). Aerosol number concentrations ($\# \text{ cm}^{-3}$) in the nuclei ($d_a < 100 \text{ nm}$) and accumulation ($100\text{--}2000 \text{ nm}$) modes. Histograms of the precipitation rates (mm h^{-1}) at the two measurement sites (b and d). The transparent bins indicate precipitation rates less than the threshold used in this study ($< 0.5 \text{ mm h}^{-1}$).

background sites from 2013 to 2020. It should be noted that the integrated range between the SMPS and APS, where discrepancies were reported for the number concentrations, showed a smooth transition without abnormal changes. The shapes of the aerosol number size distributions from the two sites were similar to a unimodal distribution, but the mode diameters between the sites were different. For Baengnyeong, the mode diameter was ~ 103 nm, and for Jeju, it was smaller than Baengnyeong at ~ 70 nm. Typically, the ranges of the aerosols can be distinguished based on their diameters, such as the nuclei mode (< 0.1 μm), accumulation mode (0.1 – 2.0 μm), and coarse mode (> 2.0 μm) (Deng et al., 2022). The nuclei mode mainly comprises homogenous/heterogeneous nucleation processes from vehicle emissions and/or volatile organic compounds (VOCs) (Seinfeld and Pandis, 2016; Venkataraman et al., 1994); high-concentration events resulting from nuclei mode aerosols are usually observed near major emission sources, such as expressways and roadsides, but their concentrations rapidly decrease with increasing distances from the emission sources (Park and Yu, 2018; Zhu et al., 2002).

Most of the aerosols in the accumulation mode are secondary aerosols (e.g., NH_4NO_3 , $(\text{NH}_4)_2\text{SO}_4$, secondary organic aerosols) that are produced by photochemical reactions with the primary aerosols emitted from combustion pollutants and gas-to-particle conversion processes. Accordingly, the high number concentration in the nuclei mode at Jeju could be from primary emission sources, especially vehicle exhaust, which has a slightly stronger impact than that for Baengnyeong. On the other hand, Baengnyeong is considered to have a relatively high number concentration in the accumulation mode because of active secondary formation with long-range pollutants transported from the Chinese mainland (Lee et al., 2015). Therefore, the aerosol number size distributions differ between the regional background sites as they are influenced by the frequency and intensity of the nucleation and growth events as well as by the transported aerosols from the regions of various sources (Jeong et al., 2010; Kim et al., 2016).

3.2. Time series of number concentrations and precipitation rates

Fig. 3a and c show the time series of average monthly aerosol number concentrations in the nuclei and accumulation modes in Baengnyeong and Jeju as well as the monthly cumulative precipitation rates observed from the nearby ASOS and AWS, respectively. The number concentrations of the nuclei and accumulation modes of Baengnyeong and Jeju were both lowest in late summer and August when the wet removal process was active because of heavy rainfall. On the other hand, the highest number concentrations were observed in October, followed by December and November, owing to increased heating fuel consumption along with shallow mixing heights as well as low precipitation (Choi and Ghim, 2016; Kim et al., 2007; Kim et al., 2012) and/or long-range transport from China. As aforementioned, the number concentration in the nuclei mode at Jeju was higher than that at Baengnyeong; thus, the difference in number concentrations between the nuclei and accumulation modes in Jeju was much smaller than that at Baengnyeong. This is attributed to the fact that the differences were mainly determined by the number concentrations in the nuclei mode along with relatively constant variations of the accumulation mode. The differences in the number concentrations between the nuclei and accumulation modes were lower in summer and winter but higher in spring and fall as the number of visitors to Jeju increased (especially near the golf courses). This result reflects that local emissions from human activities may partly influence the intensive measurement station in Jeju.

In general, large amounts of precipitation are noted in July and August (monsoon season) in Korea, and there is sporadic precipitation in the other seasons. Therefore, the precipitation conditions at both Baengnyeong and Jeju are suitable for investigating various types of precipitation, including large (intensified rainfall) and small amounts of general precipitation. The correlation coefficient (R) of the monthly average aerosol number concentration with the precipitation rate was

-0.67 , confirming that the removal effect was mainly controlled by precipitation.

Fig. 3b and d are histograms of the hourly precipitations. The numbers of precipitation cases exceeding or equal to the threshold (0.5 mm h^{-1}) are 1314 in Baengnyeong and 4151 in Jeju, respectively accounting for about 1.9% and 5.9% of the theoretically measurable 70,128 cases. The range of 0.5 – 1 mm h^{-1} accounts for about 50.6% and 43% of the total precipitation cases in Baengnyeong and Jeju, respectively, and the precipitation cases ≥ 1.0 mm h^{-1} account for $\sim 50\%$ among the considered precipitation cases (≥ 0.5 mm h^{-1}). The monthly mean precipitation rates at Baengnyeong and Jeju were 58 mm month^{-1} and 143 mm month^{-1} , respectively. The reason for the lower precipitation at Baengnyeong is that Jeju has characteristics of high precipitation, cloud cover, total column cloud water, and low cloud bottom height, suggesting higher exposure time for the wet removal process (Choi et al., 2020b). The median hourly precipitation rates at Baengnyeong and Jeju were 1.5 mm h^{-1} and 1.0 mm h^{-1} , respectively, accounting for the cases ≥ 0.5 mm h^{-1} . Compared to previous studies, the median values at the two sites are similar to or higher than 0.8 mm h^{-1} as noted by Laakso et al. (2003) and 1.57 mm h^{-1} as noted by Pryor et al. (2016) within a similar range of precipitation.

3.3. Characteristics of the below-cloud scavenging coefficient (Λ_{below})

Fig. 4a and c show the histograms of Λ_{below} based on the total number concentrations depending on the precipitation rates using Eq. (3) during the measurement periods at the two sites. The standard error of the mean for Λ_{below} ($\Delta\Lambda$) is derived as Eq. (4):

$$\Delta\Lambda = \frac{\sigma}{\sqrt{N}} \quad (4)$$

where σ is the standard deviation and N is the number of observations. The variations among all Λ_{below} (regardless of size) with 95% confidence level (mean $\Lambda_{\text{below}} \pm 2\Delta\Lambda$) ranged from $2.16 \times 10^{-5} \text{ s}^{-1}$ to $2.33 \times 10^{-5} \text{ s}^{-1}$. This narrow range indicates that the estimation has reasonably small error intervals based on the sufficiently large number of observations. Nevertheless, Λ_{below} values within the 95% confidence interval ($-4.66 \times 10^{-4} \text{ s}^{-1}$ to $5.11 \times 10^{-4} \text{ s}^{-1}$) were selected to reduce bias from the outliers by applying the criterion (mean $\Lambda \pm 2\sigma$).

Although the mean and median Λ_{below} converge within narrow ranges, the median Λ_{below} is used instead of the mean Λ_{below} because it is less sensitive to extreme or abnormal values resulting from measurement uncertainties. Although a considerable portion of the Λ_{below} values is close to (or less than) zero, the median Λ_{below} is significantly farther from zero and positive values. The reasons for these negative Λ_{below} values might be the uncertainties in the aerosol number size distribution measurements and inclusion cases of the aerosol number size distributions for non-stationary events (although these events passed the criteria for data screening) (Choi et al., 2020b; Laakso et al., 2003; Pryor et al., 2016; Zikova and Zdimal, 2016). The empirical cumulative density function of Λ_{below} derived from the corresponding rain events with 107 bin diameter (SMPS and APS) indicates that the median values of Λ_{below} were $8.06 \times 10^{-6} \text{ s}^{-1}$ (-2.13×10^{-5} to $3.70 \times 10^{-4} \text{ s}^{-1}$) for Baengnyeong and $1.04 \times 10^{-5} \text{ s}^{-1}$ (-3.42×10^{-5} to $5.33 \times 10^{-4} \text{ s}^{-1}$) for Jeju. The difference in Λ_{below} between the two sites was relatively smaller ($\sim 23\%$) than that for the precipitation rates ($\sim 43\%$). The median Λ_{below} in this study was comparable to that derived from long-term measurements over East Asia, i.e., $7.96 \times 10^{-6} \text{ s}^{-1}$ (-1.7×10^{-5} to $5.3 \times 10^{-5} \text{ s}^{-1}$) (Choi et al., 2020b). However, the median Λ_{below} is lower than previously reported values based on measurements, compared to the $1.3 \times 10^{-5} \text{ s}^{-1}$ reported by Laakso et al. (2003) and $1.9 \times 10^{-5} \text{ s}^{-1}$ noted by Pryor et al. (2016). This may be attributed to differences in the precipitation rates, precipitation drop sizes, aerosol chemical properties, aerosol hygroscopic properties, and aerosol size distributions at the measurement sites.

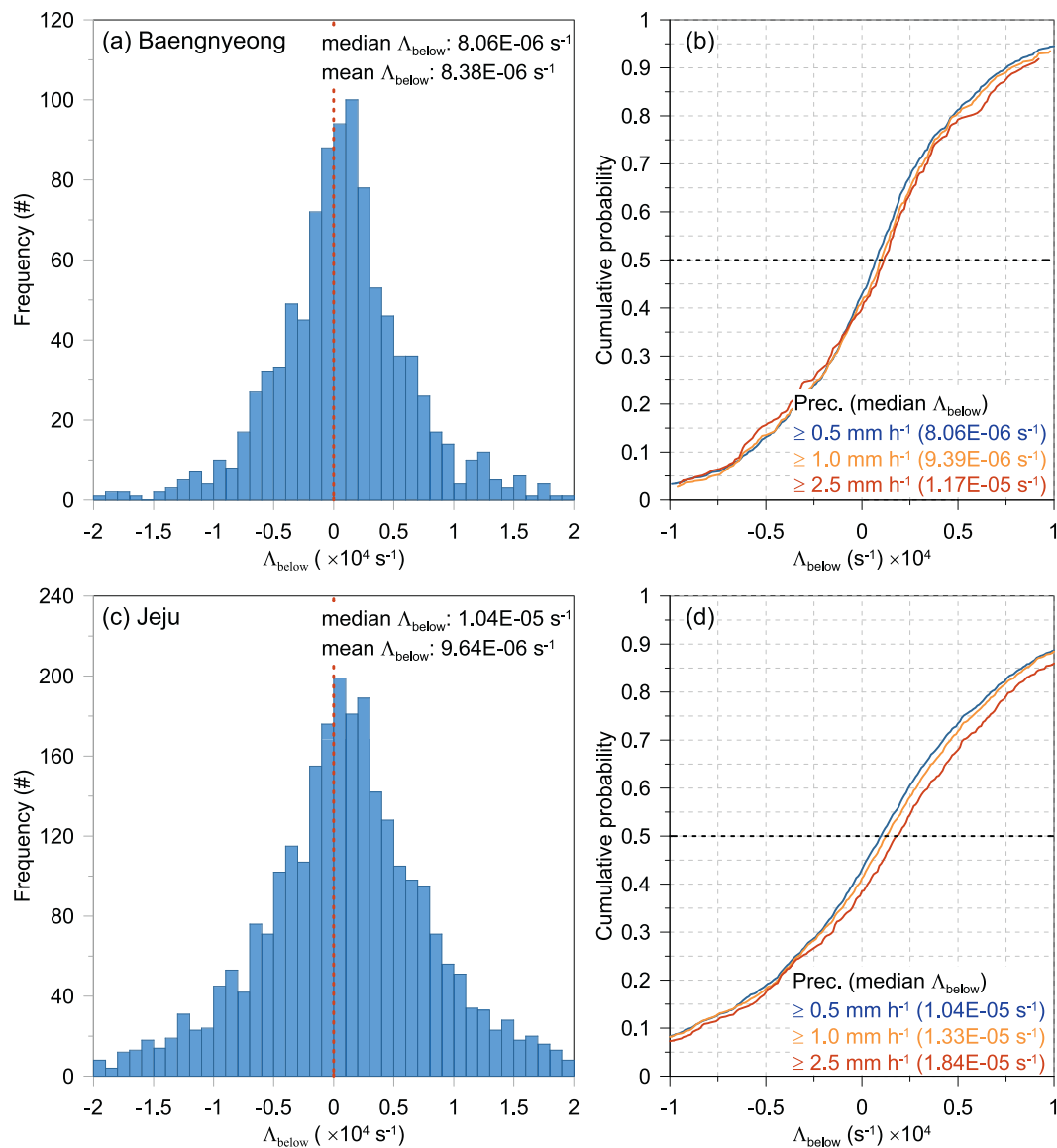


Fig. 4. Empirical cumulative distribution plots of the below-cloud scavenging coefficients (Λ_{below}) from the total number concentrations at (a) Baengnyeong and (c) Jeju. The cumulative distributions of the Λ_{below} values depending on three different precipitation rates (in mm h^{-1}) at (b) Baengnyeong and (d) Jeju are also shown. The numbers in the parentheses are the median values of Λ_{below} for the corresponding precipitation rates.

Fig. 4b and d show the cumulative frequency histograms of Λ_{below} with respect to the precipitation bins. As the threshold of the precipitation rate increases from 0.5 mm h^{-1} (all cases) to 1.0 mm h^{-1} (median), Λ_{below} values increase by factors of 1.17 and 1.27, i.e., $9.39 \times 10^{-6} \text{ s}^{-1}$ ($-2.07 \times 10^{-5} \text{ s}^{-1}$ to $4.00 \times 10^{-5} \text{ s}^{-1}$) for Baengnyeong and $1.33 \times 10^{-5} \text{ s}^{-1}$ ($-3.26 \times 10^{-5} \text{ s}^{-1}$ to $5.81 \times 10^{-5} \text{ s}^{-1}$) for Jeju, respectively. The increase in Λ_{below} is more obvious at 2.5 mm h^{-1} (75th percentile) as $1.17 \times 10^{-5} \text{ s}^{-1}$ ($-2.93 \times 10^{-5} \text{ s}^{-1}$ to $4.06 \times 10^{-5} \text{ s}^{-1}$) for Baengnyeong and $1.84 \times 10^{-5} \text{ s}^{-1}$ ($-3.04 \times 10^{-5} \text{ s}^{-1}$ to $6.68 \times 10^{-5} \text{ s}^{-1}$) for Jeju. The range of the median Λ_{below} is in good agreement with previously reported theoretical predictions (Wang et al., 2010, 2014) and experimental research (Andronache et al., 2006; Laakso et al., 2003; Pryor et al., 2016; Wang et al., 2010), suggesting that the proposed approach is reasonable. Using these obvious increasing tendencies of Λ_{below} depending on the precipitation rates, the empirical fitting equation was determined by investigating the relationship between the median Λ_{below} and precipitation rate bins.

Thus, the size-resolved Λ_{below} , which is a function of the aerosol size and precipitation intensity, was calculated according to the method of Laakso et al. (2003). First, Λ_{below} was calculated as a running median of

three-bin channels. The precipitation intensities were then divided into four intensity classes corresponding to the following precipitation rates: between 0.5 and 1 mm h^{-1} , between 1 and 2 mm h^{-1} , between 2 and 5 mm h^{-1} , and $\geq 5 \text{ mm h}^{-1}$. Clear differences were found between the different precipitation intensities as the medians for these four groups were 0.5 , 1.0 , 2.9 , and 6.5 mm h^{-1} , respectively. It should be noted that the median and mean values of Λ_{below} did not significantly differ from each other systematically and that the median has less variation, which is suitable for deriving the empirical equation (Fig. 5a). The variation of Λ_{below} based on aerosol size shows a negative quadratic curve shape, indicating that Λ_{below} is high at small and large diameters along with a local minimum value at $\sim 70 \text{ nm}$. Laakso et al. (2003) also reported a similar size-resolved variation as the result of this work but their local minimum was observed at 200 nm , which is higher than that in this study (Fig. 5b). This may be attributed to the regional differences in the aerosol and precipitation characteristics; therefore, this relationship between Λ_{below} and aerosol size depending on the precipitation rate may be considered reasonable for the characteristics of the Korean peninsula because it is derived from sufficient long-term data of >8 years.

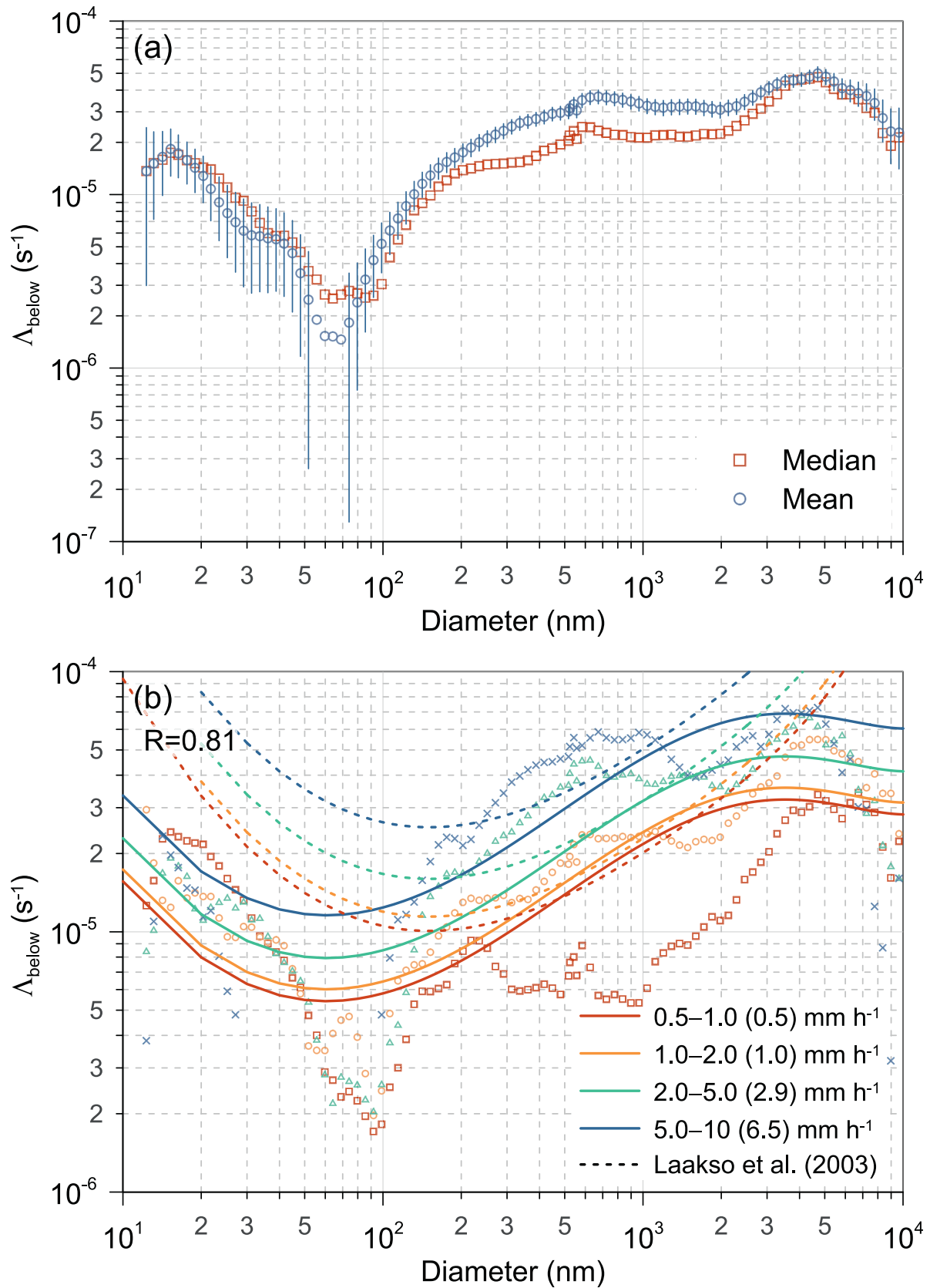


Fig. 5. (a) Mean (blue) with error bar ($2\Delta\Lambda$) and median (red) values of the below-cloud scavenging coefficients (Λ_{below}) as functions of the aerosol diameter (d_a) from the combined data at Baengnyeong and Jeju. (b) Variation in the size-resolved median Λ_{below} according to the precipitation rate (different colored symbols). The solid curved lines are derived from the fitting procedure using averages over three adjacent size bins. The dashed lines denote the results of parameterization by Laakso et al. (2003) for the corresponding median precipitation rates in each of the bins. (For interpretation of the references to colour in this figure legend, the reader is referred to the web version of this article.)

3.4. Size-resolved below-cloud scavenging coefficient (Λ_{below})

Based on the characteristics of the size-resolved Λ_{below} according to the precipitation rates described in Section 3.3, Λ_{below} was parameterized as a function of the aerosol diameter and precipitation rate as per the works of Laakso et al. (2003) and Pryor et al. (2016) using Eq. (5):

$$\log(\Lambda_{\text{below}}) = a + b \cdot d_a^{-4} + c \cdot d_a^{-3} + d \cdot d_a^{-2} + e \cdot d_a^{-1} + f \cdot \sqrt{p} \quad (5)$$

A fourth-degree polynomial equation was derived with fitting parameters (a to f), and the units of d_a and p were μm and mm h^{-1} , respectively (Table 1). Although the fitted Λ_{below} exhibits discrepancies with not only the observed Λ_{below} but also the values reported by Laakso et al. (2003) and Pryor et al. (2016), the correlation coefficient in this study is higher (0.81) than the value of 0.68 reported by Pryor et al. (2016), indicating good agreement between the two Λ_{below} values (Fig. 5b). As the precipitation rate increased, the fitted Λ_{below} curve also increased smoothly, suggesting that the derived parameterization was captured adequately as a function of the precipitation rate. The root mean squared error (RMSE) between the fitted and observed Λ_{below} was slightly lower ($1.05 \times 10^{-5} \text{ s}^{-1}$) than that reported by Pryor et al. (2016) ($1.23 \times 10^{-5} \text{ s}^{-1}$ to $1.63 \times 10^{-5} \text{ s}^{-1}$). It should be noted that the parameterizations in previous studies were based on data points measured for aerosols in the size range of 10–500 nm; thus, values for aerosols exceeding sizes of 500 nm were estimated using the all-too-common extrapolation approach for different kinds of parameterizations (Laakso et al., 2003). On the other hand, the derived parameterization covers the range from 10 nm to 10 μm and avoids overestimation by extrapolation of Λ_{below} for aerosol diameters above 500 nm. For these reasons, the shape of Λ_{below} depending on the aerosol diameter was different between this study and Laakso et al. (2003) for diameters larger than 500 nm; Λ_{below} from Laakso et al. (2003) increased continuously as the aerosol size increased, whereas Λ_{below} in this study was relatively constant at $d_a > \sim 1 \mu\text{m}$, similar to the shape derived from the theoretical equation (Slinn, 1983; Wang et al., 2014).

To compare the magnitudes of Λ_{below} derived from long-term observation data, the values of Λ_{below} using parameters from previous studies (Table 1) based on measured data were calculated by assuming that the aerosol diameters were approximately 200 and 500 nm (Fig. 6). It should be noted that Λ_{below} from the other schemes are not shown in Fig. 6 because these were either too high or low compared to the obtained Λ_{below} (Choi et al., 2020b). The mean fractional bias (MFB; $2 \times [A - B]/[A + B]$) is used herein, where A and B denote Λ_{below} from the previous and present study, respectively. At 200 nm, the obtained Λ_{below} values were comparable with those reported by Laakso et al. (2003) but slightly higher than the obtained Λ_{below} , with the MFB ranging from 0.25 to 0.62. However, Λ_{below} from Choi et al. (2020b) and Pryor et al. (2016) were much higher than the obtained Λ_{below} by one order of magnitude, indicating that these studies assumed that larger amounts of aerosols with diameters of 200 nm were easily removed from the atmosphere. When the aerosol diameter increased to 500 nm, Λ_{below} from Laakso et al. (2003) still showed fairly good agreement with the obtained Λ_{below} but the MFB ranged from -0.06 to 0.33 . The MFB was negative at low precipitation rates, but the opposite tendency was observed for precipitation rates of $\sim 3 \text{ mm h}^{-1}$. Consequently, the magnitude of Λ_{below} from Laakso et al. (2003) was generally lower when considering that the median precipitation rates at Baengnyeong and Jeju were 1.5 mm h^{-1} and 1.0 mm h^{-1} , respectively.

Table 1

Fitting parameters for the fourth-degree polynomial equation ($\log(\Lambda_{\text{below}}) = a + b \cdot d_a^{-4} + c \cdot d_a^{-3} + d \cdot d_a^{-2} + e \cdot d_a^{-1} + f \cdot \sqrt{p}$). The units for d_a and p are μm and mm h^{-1} , respectively.

	a	b	c	d	e	f
This study	288.016	325,031	230,342	60,366.0	6924.56	0.200145
Laakso et al. (2003)	274.36	332,839.6	226,656	58,005.9	6588.38	0.24498
Pryor et al. (2016)	3454.908	10,040,252	5,484,421	1,121,475	101,768.6	0.185

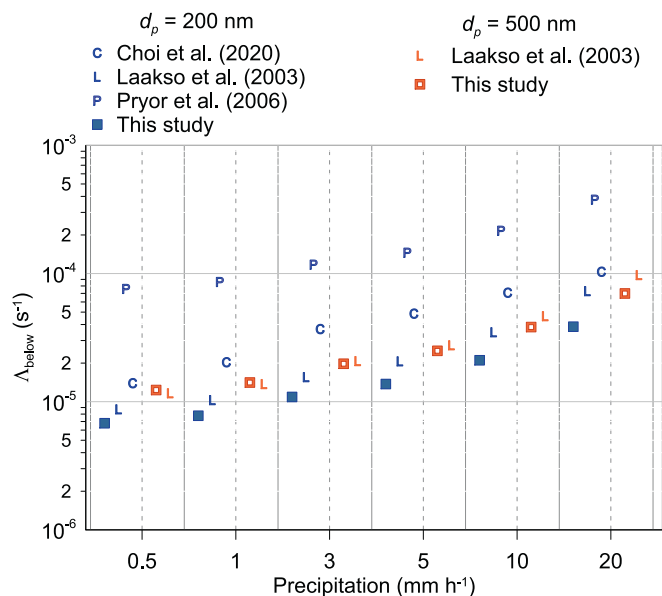


Fig. 6. Variations in the calculated and measured below-cloud scavenging coefficients (Λ_{below} ; s^{-1}) depending on the precipitation rates (mm h^{-1}). The blue and orange symbols depict the results from the size-resolved Λ_{below} equation based on assumed diameters of 200 and 500 nm, respectively. (For interpretation of the references to colour in this figure legend, the reader is referred to the web version of this article.)

4. Summary and conclusions

Owing to insufficient *in-situ* detailed observations to explain and quantify the wet scavenging coefficient (Λ), it is a challenging task to predict accurate aerosol concentrations and/or effects in the atmosphere. Among the wet scavenging processes (below- and in-cloud), below-cloud scavenging has been identified as one of the most efficient removal mechanisms for atmospheric aerosols. Because the below-cloud scavenging coefficient (Λ_{below}) shows large spatial and temporal variations resulting from differences in factors, such as precipitation types, aerosol chemical compositions, and aerosol size distributions, this study focused on establishing an empirical equation for the size-resolved Λ_{below} for the first time using long-term data measurements (8 years) by combining the aerosol number size concentrations and meteorological variables at two background sites in Korea (Baengnyeong and Jeju).

The shapes of the aerosol number size distributions from the two sites were similar to a unimodal distribution, but the mode diameters between the two sites were different; the mode diameters at Baengnyeong and Jeju were $\sim 70 \text{ nm}$ (nuclei mode) and $\sim 103 \text{ nm}$ (accumulation mode), respectively. This is because the conditions in Jeju could be influenced by its primary emission sources (vehicle exhaust), whereas the conditions in Baengnyeong are mainly affected by active secondary formation with long-range pollutants transported from the Chinese mainland. The number concentrations of the nuclei and accumulation modes in both Baengnyeong and Jeju were lowest in late summer and August and started increasing in October owing to the active wet removal process caused by heavy rainfall and increase in the local emissions and/or long-range transport from China.

The empirical cumulative density functions of Λ_{below} derived from the total number concentrations using the corresponding rain events indicate that the median values of Λ_{below} from the two sites were $8.06 \times 10^{-6} \text{ s}^{-1}$ for Baengnyeong and $1.04 \times 10^{-5} \text{ s}^{-1}$ for Jeju. These values are comparable to the Λ_{below} from long-term black carbon and carbon monoxide data over East Asia ($7.96 \times 10^{-6} \text{ s}^{-1}$) but lower than the values in Finland ($1.3 \times 10^{-5} \text{ s}^{-1}$) and the U.S. ($1.9 \times 10^{-5} \text{ s}^{-1}$). This may be attributed to differences in the precipitation rates, precipitation drop sizes, aerosol chemical/hygroscopic properties, and aerosol size distributions at the measurement sites. Although the proposed parameterization covers the range from 10 nm to 10 μm , the derived fourth-degree polynomial equation shows a high correlation coefficient of 0.81 than the previous study, indicating that Λ_{below} converges within a narrow range. However, the variation in Λ_{below} depending on aerosol diameter was *u*-shaped with a local minimum at ~ 70 nm and relatively constant at $d_a > \sim 1$ μm , similar to that derived from the theoretical equation. At 200 nm, the obtained Λ_{below} values were much lower than those reported in previous studies by one order of magnitude, except for the value reported by Laakso et al. (2003), indicating that these studies assumed that larger amounts of aerosols with diameters of 200 nm were easily removed from the atmosphere. When the aerosol diameter increased to 500 nm, Λ_{below} reported by Laakso et al. (2003), which showed fairly good agreement with the obtained Λ_{below} , was generally lower when considering that the median precipitation rates at the two background sites were 1 mm h⁻¹ to 1.5 mm h⁻¹, implying an active aerosol removal process over East Asia.

This study is expected to contribute toward improving the below-cloud scavenging modules implemented in chemical transport models by covering a wide range of aerosol diameters (10 nm to 10 μm) to avoid overestimations due to extrapolation of Λ_{below} . These results are also expected to help improve the understanding of aerosol behaviors over East Asia, especially the Korean peninsula.

CRedit authorship contribution statement

Yongjoo Choi: Conceptualization, Methodology, Investigation, Data curation, Writing – original draft. **Chang Hoon Jung:** Writing – review & editing, Funding acquisition. **Junyoung Ahn:** Conceptualization, Validation. **Seung-Myung Park:** Data curation. **Kyung Man Han:** Writing – review & editing. **Jongbyeok Jun:** Data curation. **Giyeol Lee:** Data curation. **Jiyoung Kim:** Validation. **Yongjae Lim:** Data curation. **Kyeong-Sik Kang:** Data curation. **Ilkwon Nam:** Methodology. **Sumin Kim:** Methodology.

Declaration of Competing Interest

The authors declare that they have no known competing financial interests or personal relationships that could have appeared to influence the work reported in this paper.

Data availability

Data will be made available on request.

Acknowledgments

This study was supported by the Fine Particle Research Initiative in East Asia Considering National Differences (FRIEND) project through the National Research Foundation of Korea (NRF) funded by the Ministry of Science and ICT (grant number 2020M3G1A1114617). The additional data analysis was supported by the National Institute of Environmental Research (NIER-2022-04-02-103).

References

- Andronache, C., 2003. Estimated variability of below-cloud aerosol removal by rainfall for observed aerosol size distributions. *Atmos. Chem. Phys.* 3, 131–143.
- Andronache, C., Grönholm, T., Laakso, L., Phillips, V., Venäläinen, A., 2006. Scavenging of ultrafine particles by rainfall at a boreal site: observations and model estimations. *Atmos. Chem. Phys.* 6, 4739–4754.
- Baklanov, A., Sorensen, J.H., 2001. Parameterisation of radionuclide deposition in atmospheric long-range transport modelling. *Phys. Chem. Earth, Part B: Hydrol., Oceans Atmosp.* 26, 787–799.
- Baron, P.A., 1986. Calibration and use of the Aerodynamic Particle Sizer (APS 3300). *Aerosol Sci. Technol.* 5, 55–67.
- Beddows, D.C.S., Dall'Osto, M., Harrison, R.M., 2009. Cluster Analysis of Rural, Urban, and Curbside Atmospheric Particle Size Data. *Environ. Sci. Technol.* 43, 4694–4700.
- Blanco-Alegre, C., et al., 2018. Below-cloud scavenging of fine and coarse aerosol particles by rain: the role of raindrop size. *Q. J. R. Meteorol. Soc.* 144, 2715–2726.
- Blanco-Alegre, C., et al., 2021. Scavenging of submicron aerosol particles in a suburban atmosphere: the raindrop size factor. *Environ. Pollut.* 285, 117371.
- Boris, A.J., et al., 2016. Fog composition at Baengnyeong Island in the eastern Yellow Sea: detecting markers of aqueous atmospheric oxidations. *Atmos. Chem. Phys.* 16, 437–453.
- Chakraborty, A., Gupta, T., Tripathi, S.N., 2016. Chemical composition and characteristics of ambient aerosols and rainwater residues during Indian summer monsoon: Insight from aerosol mass spectrometry. *Atmos. Environ.* 136, 144–155.
- Chate, D.M., et al., 2003. Scavenging of aerosols and their chemical species by rain. *Atmos. Environ.* 37, 2477–2484.
- Chatterjee, A., Jayaraman, A., Rao, T.N., Raha, S., 2010. In-cloud and below-cloud scavenging of aerosol ionic species over a tropical rural atmosphere in India. *J. Atmos. Chem.* 66, 27–40.
- Choi, Y., Ghim, Y.S., 2016. Estimation of columnar concentrations of absorbing and scattering fine mode aerosol components using AERONET data. *J. Geophys. Res.-Atmos.* 121.
- Choi, Y., et al., 2020a. Regional variability in black carbon and carbon monoxide ratio from long-term observations over East Asia: assessment of representativeness for black carbon (BC) and carbon monoxide (CO) emission inventories. *Atmos. Chem. Phys.* 20, 83–98.
- Choi, Y., et al., 2020b. Investigation of the wet removal rate of black carbon in East Asia: validation of a below- and in-cloud wet removal scheme in FLEXible PARTicle (FLEXPART) model v10.4. *Atmos. Chem. Phys.* 20, 13655–13670.
- Croft, B., et al., 2010. Influences of in-cloud aerosol scavenging parameterizations on aerosol concentrations and wet deposition in ECHAM5-HAM. *Atmos. Chem. Phys.* 10, 1511–1543.
- Cugeron, K., De Michele, C., Ghezzi, A., Gianelle, V., 2018. Aerosol removal due to precipitation and wind forcings in Milan urban area. *J. Hydrol.* 556, 1256–1262.
- Deng, C., et al., 2022. Measurement report: size distributions of urban aerosols down to 1 nm from long-term measurements. *Atmos. Chem. Phys.* 22, 13569–13580.
- Ding, S., et al., 2019. Observed Interactions between Black Carbon and Hydrometeor during Wet Scavenging in Mixed-phase Clouds. *Geophys. Res. Lett.* 46, 8453–8463.
- Feng, J., 2007. A 3-mode parameterization of below-cloud scavenging of aerosols for use in atmospheric dispersion models. *Atmos. Environ.* 41, 6808–6822.
- Ge, B., et al., 2021. Inter-annual variations of wet deposition in Beijing from 2014–2017: implications of below-cloud scavenging of inorganic aerosols. *Atmos. Chem. Phys.* 21, 9441–9454.
- Grythe, H., et al., 2017. A new aerosol wet removal scheme for the Lagrangian particle model FLEXPART v10. *Geosci. Model Dev.* 10, 1447–1466.
- Henzing, J.S., Olivé, D.J.L., van Velthoven, P.F.J., 2006. A parameterization of size resolved below cloud scavenging of aerosols by rain. *Atmos. Chem. Phys.* 6, 3363–3375.
- Hu, M., Zhang, J., Wu, Z., 2005. Chemical compositions of precipitation and scavenging of particles in Beijing. *Sci. China Series B Chem.* 48, 265–272.
- Jeong, C.H., et al., 2010. Particle formation and growth at five rural and urban sites. *Atmos. Chem. Phys.* 10, 7979–7995.
- Jones, A.C., et al., 2022. Below-cloud scavenging of aerosol by rain: a review of numerical modelling approaches and sensitivity simulations with mineral dust in the Met Office's Unified Model. *Atmos. Chem. Phys.* 22, 11381–11407.
- Jung, C.H., et al., 2022. Parameterization of below-cloud scavenging for polydisperse fine mode aerosols as a function of rain intensity. *J. Environ. Sci.* 132, 43–55.
- Jylhä, K., 1991. Empirical scavenging coefficients of radioactive substances released from Chernobyl. *Atmos. Environ. Part A* 25, 263–270.
- Khlystov, A., Stanier, C., Pandis, S.N., 2004. An Algorithm for Combining Electrical Mobility and Aerodynamic size Distributions Data when measuring Ambient Aerosol special issue of Aerosol Science and Technology on Findings from the Fine Particulate Matter Supersites Program. *Aerosol Sci. Technol.* 38, 229–238.
- Kim, H.-S., Huh, J.-B., Hopke, P.K., Holsen, T.M., Yi, S.-M., 2007. Characteristics of the major chemical constituents of PM_{2.5} and smog events in Seoul, Korea in 2003 and 2004. *Atmos. Environ.* 41, 6762–6770.
- Kim, W., Lee, H., Kim, J., Jeong, U., Kweon, J., 2012. Estimation of seasonal diurnal variations in primary and secondary organic carbon concentrations in the urban atmosphere: EC tracer and multiple regression approaches. *Atmos. Environ.* 56, 101–108.
- Kim, Y., et al., 2013. Observation of new particle formation and growth events in Asian continental outflow. *Atmos. Environ.* 64, 160–168.
- Kim, Y., et al., 2016. Characteristics of formation and growth of atmospheric nanoparticles observed at four regional background sites in Korea. *Atmos. Res.* 168, 80–91.

- Laakso, L., et al., 2003. Ultrafine particle scavenging coefficients calculated from 6 years field measurements. *Atmos. Environ.* 37, 3605–3613.
- Lee, T., et al., 2015. Characterization of aerosol composition, concentrations, and sources at Baengnyeong Island, Korea using an aerosol mass spectrometer. *Atmos. Environ.* 120, 297–306.
- Lee, Y., Choi, Y., An, H., Park, J., Ghim, Y.S., 2021. Cluster analysis of atmospheric particle number size distributions at a rural site downwind of Seoul, Korea. *Atmosph. Pollut. Res.* 12, 101086.
- Luo, G., Yu, F., Schwab, J., 2019. Revised treatment of wet scavenging processes dramatically improves GEOS-Chem 12.0.0 simulations of surface nitric acid, nitrate, and ammonium over the United States. *Geosci. Model Dev.* 12, 3439–3447.
- Luo, G., Yu, F., Moch, J.M., 2020. Further improvement of wet process treatments in GEOS-Chem v12.6.0: impact on global distributions of aerosols and aerosol precursors. *Geosci. Model Dev.* 13, 2879–2903.
- Park, S., Yu, G.-H., 2018. Effect of Air Stagnation Conditions on Mass size Distributions of Water-soluble Aerosol Particles. *J. Korean Soc. for Atmos. Environ.* 34, 418–429.
- Park, T., et al., 2022. Characterization of chemical and physical changes in atmospheric aerosols during fog processing at Baengnyeong Island, South Korea. *Atmos. Environ.* 278, 119091.
- Pryor, S.C., Joerger, V.M., Sullivan, R.C., 2016. Empirical estimates of size-resolved precipitation scavenging coefficients for ultrafine particles. *Atmos. Environ.* 143, 133–138.
- Rajeev, P., Rajput, P., Gupta, T., 2016. Chemical characteristics of aerosol and rain water during an El Niño and PDO influenced Indian summer monsoon. *Atmos. Environ.* 145, 192–200.
- Rissler, J., et al., 2014. Effective Density and Mixing State of Aerosol Particles in a Near-Traffic Urban Environment. *Environ. Sci. Technol.* 48, 6300–6308.
- Ryu, Y.-H., Min, S.-K., 2022. Improving Wet and Dry Deposition of Aerosols in WRF-Chem: Updates to Below-Cloud Scavenging and Coarse-Particle Dry Deposition. *J. Advan. Model. Earth Syst.* 14 e2021MS002792.
- Seinfeld, J.H., Pandis, S.N., 2016. *Atmospheric Chemistry and Physics: From Air Pollution to Climate Change*. John Wiley & Sons.
- Si, M., et al., 2018. Ice-nucleating ability of aerosol particles and possible sources at three coastal marine sites. *Atmos. Chem. Phys.* 18, 15669–15685.
- Slinn, W., 1983. Precipitation scavenging. In: *Atmospheric Sciences and Power Production-1979*, Division of Biomedical Environmental Research. US Department of Energy, Washington, DC, pp. 466–532.
- Textor, C., et al., 2006. Analysis and quantification of the diversities of aerosol life cycles within AeroCom. *Atmos. Chem. Phys.* 6, 1777–1813.
- Venkataraman, C., Lyons, J.M., Friedlander, S.K., 1994. *Size Distributions of Polycyclic Aromatic Hydrocarbons and Elemental Carbon. 1. Sampling, Measurement Methods, and Source Characterization*. *Environ. Sci. Technol.* 28, 555–562.
- Wang, X., Zhang, L., Moran, M.D., 2010. Uncertainty assessment of current size-resolved parameterizations for below-cloud particle scavenging by rain. *Atmos. Chem. Phys.* 10, 5685–5705.
- Wang, X., Zhang, L., Moran, M.D., 2011. On the discrepancies between theoretical and measured below-cloud particle scavenging coefficients for rain – a numerical investigation using a detailed one-dimensional cloud microphysics model. *Atmos. Chem. Phys.* 11, 11859–11866.
- Wang, X., Zhang, L., Moran, M.D., 2014. Development of a new semi-empirical parameterization for below-cloud scavenging of size-resolved aerosol particles by both rain and snow. *Geosci. Model Dev.* 7, 799–819.
- Wu, Y., et al., 2022. The wet scavenging of air pollutants through artificial precipitation enhancement: a case study in the Yangtze River Delta. *Front. Environ. Sci.* 10.
- Xu, D., et al., 2017. Below-cloud wet scavenging of soluble inorganic ions by rain in Beijing during the summer of 2014. *Environ. Pollut.* 230, 963–973.
- Xu, D., et al., 2019. Multi-method determination of the below-cloud wet scavenging coefficients of aerosols in Beijing, China. *Atmos. Chem. Phys.* 19, 15569–15581.
- Zhang, L., Wang, X., Moran, M.D., Feng, J., 2013. Review and uncertainty assessment of size-resolved scavenging coefficient formulations for below-cloud snow scavenging of atmospheric aerosols. *Atmos. Chem. Phys.* 13, 10005–10025.
- Zhu, Y., Hinds, W.C., Kim, S., Shen, S., Sioutas, C., 2002. Study of ultrafine particles near a major highway with heavy-duty diesel traffic. *Atmos. Environ.* 36, 4323–4335.
- Zikova, N., Zdimal, V., 2016. Precipitation scavenging of aerosol particles at a rural site in the Czech Republic. *Tellus Ser. B Chem. Phys. Meteorol.* 68, 27343.